

# From Occlusion to Insight: Object Search in Semantic Shelves using Large Language Models

Satvik Sharma<sup>\*1</sup>, Kaushik Shivakumar<sup>\*1</sup>, Huang Huang<sup>\*1</sup>, Ryan Hoque<sup>1</sup>, Alishba Imran<sup>1</sup>, Brian Ichter<sup>2</sup>, Ken Goldberg<sup>1</sup>

**Abstract**—How can a robot efficiently extract a desired object from a shelf when it is fully occluded by other objects? Prior works propose geometric approaches for this problem but do not consider object semantics. Shelves in pharmacies, restaurant kitchens, and grocery stores are often organized such that semantically similar objects are placed close to one another. Can large language models (LLMs) serve as semantic knowledge sources to accelerate robotic mechanical search in semantically arranged environments? With Semantic Spatial Search on Shelves ( $S^4$ ), we use LLMs to generate affinity matrices, where entries correspond to semantic likelihood of physical proximity between objects. We derive semantic spatial distributions by synthesizing semantics with learned geometric constraints.  $S^4$  incorporates Optical Character Recognition (OCR) and semantic refinement with predictions from ViLD, an open-vocabulary object detection model. Simulation experiments suggest that semantic spatial search reduces the search time relative to pure spatial search by an average of 24% across three domains: pharmacy, kitchen, and office shelves. A manually collected dataset of 100 semantic scenes suggests that OCR and semantic refinement improve object detection accuracy by 35%. Lastly, physical experiments in a pharmacy shelf suggest 47.1% improvement over pure spatial search. Supplementary material can be found at this website.

## I. INTRODUCTION

Robotic mechanical search [9] aims to retrieve a desired target object from a scene where the target object is fully occluded. This problem is especially challenging in shelves due to limited camera views and robot access. However, these environments are often organized semantically for ease of retrieval. For instance, pain relief medications such as Tylenol and Ibuprofen are often stored near each other. Can the semantic structure of an environment guide mechanical search by informing the robot about what areas are likely to contain the target object? Prior work in mechanical search either fails to consider semantic information [20, 21, 22] or uses manually constructed semantic similarities [25].

In this paper, we propose using large language models (LLMs) [10, 15] as semantic knowledge bases for guiding robotic mechanical search. Since LLMs are trained on large corpora of human language, we hypothesize that they effectively encode the semantics of both common and rare objects. In contrast to recent systems like SayCan [18], we apply LLMs offline to facilitate searching and manipulating cluttered shelf environments where many objects are fully occluded. We generate an *occupancy distribution*, a probability distribution



Fig. 1: (A) Consider a robot search for a target object such as Tylenol in a semantically arranged environment such as a pharmacy shelf. (B) Semantic Spatial Search on Shelves ( $S^4$ ) computes a *spatial distribution* and a *semantic distribution* (see shaded areas) over where the target object could be. The spatial distribution is based on object shapes while the semantic distribution encodes likelihood of physical proximity (e.g., Tylenol is likely closest to Ibuprofen). (C) These are combined into a single *semantic spatial distribution*.

over the potential locations of the target object. We develop a novel method to estimate a *semantic occupancy distribution* by precomputing an affinity matrix from an LLM. The semantic affinity matrix consists of many rows, where values in row  $i$  encode physical proximity of every object to object  $i$ . We combine the semantic occupancy distribution with a learned spatial occupancy distribution which encodes constraints due to object geometry and camera perspective, shown to be helpful in prior work [21, 22] (Figure 1). We then use the

<sup>1</sup>AUTOLAB at the University of California, Berkeley

<sup>2</sup>Google Brain

\*equal contribution

resulting semantic spatial distribution to efficiently search in the target domain.

Since generating a semantic distribution requires objects in the shelf to be identified correctly, we use object detection and segmentation to identify objects in the shelf. To improve performance, we refine the object detection class probabilities to more accurately identify heavily occluded objects and distinguish between visually similar objects (e.g., shampoo and conditioner), in two ways: 1) by extracting brand names or labels from the images through Optical Character Recognition (OCR), and 2) by using clues from nearby, more confident object detections to refine detections. Hence, we apply LLMs to improving object detection without any additional annotated data, which is often required to deploy object detection models in robotics. We find that OCR with an off-the-shelf text embedding model combined with context-based semantic refinement with LLMs significantly improves object detection.

Existing product taxonomies such as the open-source Google Product Taxonomy [5] provide semantic context for objects, but they have a limited vocabulary and mostly consist of categories (e.g., “supplements”) rather than specific products (e.g., “Omega-3”). In this work, we evaluate our method in the pharmacy, kitchen, and office domains indexed in the Google Product Taxonomy, which we treat as ground truth for generating semantically organized scenes and evaluating affinity matrices.

This paper makes the following contributions:

- 1) A novel approach for synthesizing semantic affinity matrices from offline LLM queries.
- 2) A systematic comparison of BERT [10], CLIP [32], OpenAI Embeddings [13], OPT-13B [16], and PaLM with the Google Product Taxonomy for inferring the semantic similarity of pharmacy products.
- 3) Semantic Spatial Search on Shelves ( $S^4$ ), a novel algorithm that combines object semantics with geometric constraints to guide mechanical search.
- 4) A method for refining the predictions of an off-the-shelf object detection model using Optical Character Recognition (OCR) and context using LLMs.
- 5) Simulation and physical experiments evaluating  $S^4$  with and without semantics, OCR, and semantic arrangement of shelves.  $S^4$  outperforms prior work by 24% in the simulated pharmacy, kitchen, and office domains and 47.1% in the physical experiments for the pharmacy domain.

## II. PRELIMINARIES AND RELATED WORK

### A. Large Language Models

Language models (LMs) output probability distributions over sequences of natural language tokens  $w_1, w_2, \dots, w_n$ . LMs typically factor the probability of the sequence with the chain rule and autoregressively perform next-token prediction:  $p(w_{1..i}) = p(w_1) \cdot p(w_2|w_1) \cdots p(w_i|w_{1..i-1})$ . In recent years, the Transformer neural network architecture [37] has enabled LMs to scale to “large language models” (LLMs) that train

billions of parameters on terabytes of data, such as GPT-3 [17] and PaLM [12]. LLMs encode semantic context and have achieved state-of-the-art results on tasks such as machine translation, question answering, text generation, and text summarization [10, 17, 12].

### B. Natural Language for Robotics

Prior work at the intersection of natural language processing and robotics includes language-conditioned imitation learning [34, 29, 35, 28], language-conditioned reinforcement learning [30, 23, 31], and online correction of robot policies through language feedback [33, 8]. Liang et al. [26] use code synthesis with LLMs to write robot control policies. Ichter et al. [14] propose SayCan, which uses a LLM for high-level planning and generating associations between language instructions and robot action primitives (e.g., “pick up the sponge”). In contrast,  $S^4$  uses a LLM to create an occupancy distribution for mechanical search of fully occluded objects. Unlike SayCan,  $S^4$  queries LLMs offline (before robot execution) because LLM inference is costly in terms of both time and compute [17].

Similar to our work, Carion et al. [4] uses language models to compute affinity scores among objects for spatial scene understanding. They propose HOLM, a system for determining where objects may be in partially observable scenes based on semantics. However, HOLM is evaluated only in simulation and considers camera adjustment actions rather than physical interactions with the environment. In contrast, we use object affinities to generate a semantic occupancy distribution, a novel way to interpret the scene and integrate geometric constraints for real-world mechanical search.

### C. Robotic Mechanical Search

Much of prior work on mechanical search considers shelves, but not in semantically arranged environments [21, 22, 20, 6]. Prior work proposes the LAX-RAY system [20], which uses a neural network to predict a spatial “occupancy distribution” for where an occluded target object could be located at a given time, by considering object geometries and camera perspective effect (e.g., high target object can’t be occluded by short object and object in the center of the camera frame occludes more areas). At each timestep, the spatial occupancy distribution is updated to be the minimum of the previous distribution and the current predicted distribution. LAX-RAY proposes Distribution Area Reduction (DAR) as a search policy that specifies the sequence of lateral pushing actions to take in order to reveal the target object as quickly as possible. DAR is a greedy strategy that first moves the object whose segmentation mask maximally overlaps with the spatial occupancy distribution to an area of minimal overlap. In this work, we extend the notion of occupancy distributions to semantics and use DAR as our mechanical search policy.

Kurenkov et al. [25] consider both semantics and geometry for mechanical search. However, they manually generate semantic categories with typically 1-2 categories in the shelf, which can deviate from real world distribution. Their

approach does not scale to the complexity of real world semantics and is tested only in simulation. In contrast, we harness the knowledge of large language models to extract open-vocabulary semantic information and accelerate robotic mechanical search.

#### D. Object Detection Refinement

Accurate object detection is a critical step in many downstream robotics applications, including mechanical search. We propose using OCR and LLMs in  $S^4$  to refine object detection by considering the conditional probabilities of all the object classes given the text present on them. While OCR has been used in prior work to aid object detection [24], we use text embedding combined with OCR for better performance.  $S^4$  also uses the semantic context of nearby objects to refine object detection. There exists prior work [1, 28, 11, 7] that considers using context from surrounding regions and objects to inform object detection, but these approaches do not use large language models as semantic knowledge bases. There are some recent object detection models such as DETR [3, 36] that are based on Transformers [37] and use full scene context to detect objects. However, these models learn these relationships from scratch, which requires an extensive amount of training data. By using off-the-shelf large language models, we can provide this context without any additional data or learning from pixels.

### III. PROBLEM STATEMENT

The starting state of a scene is drawn from the space of *semantically organized* scenes, sampled proportionally to its approximate likelihood of occurrence in the real world. We base these likelihoods on the Google Product Taxonomy [5] and describe our procedure for scene generation in Section V-B.

We consider the problem of robotic mechanical search for a target object  $\mathcal{O}_T$  in a cluttered, semantically organized shelf containing the target and  $N$  other rigid objects  $\{\mathcal{O}_1, \dots, \mathcal{O}_N\}$  of cuboidal shapes in stable poses. We build on the problem statement and assumptions in Huang et al. [21]. We model the setup as a finite-horizon Partially Observable Markov Decision Process (POMDP). States  $s_t \in \mathcal{S}$  consist of the full geometries and poses of the objects in the shelf at timestep  $t$  and observations  $y_t \in \mathcal{Y} = \mathcal{R}^{H \times W \times 4}$  are RGBD images from a robot-mounted depth camera at timestep  $t$ . Actions  $a_t \in \mathcal{A} = \mathcal{A}_p \cup \mathcal{A}_s$  are either *pushing* or *suction* actions, where the former are horizontal linear translations of an object along the shelf and the latter pick up an object with a suction gripper and translate it to an empty location on the shelf with no other objects in front of it.

We make the following assumptions:

- The dimensions of the shelf are known.
- Each dimension of each object is between size  $S_{\min} = 5$  cm and size  $S_{\max} = 25$  cm.
- The shelf is semantically organized.
- The names of all objects in the shelf are a subset of a known list of object names.

- Actions cannot inadvertently topple objects or move multiple objects simultaneously.

The objective is to minimize the total number of actions required to reveal at least  $X\%$  of the target object to the camera. A trial is successful if this threshold visibility  $X$  is reached within  $H = 2N$  actions, and unsuccessful otherwise.

## IV. METHODS

### A. Affinity Matrix Generation

LLMs are best known for their ability to generate unstructured free-form text. However, in our work, we use them to provide probabilistic completions to textual prompts in order to generate an occupancy distribution encoding the semantics of any scene that may contain it along with other objects. This is possible because training data for such models contains a vast amount of information about object semantics [12, 17]. We extract this information from language models offline (i.e., before robot task execution).

We query the language model with a specific prompt: “In a shelf, the  $X$  goes next to the \_\_\_\_.” Note that this prompt queries the LLM for the notion of physical proximity rather than pure semantic similarity. We use the scoring mode of the language models to find the probabilities of each of the object names appearing in the blank space. This creates a row of the affinity matrix corresponding to object  $X$ . We iterate over all object names to create the full matrix,  $M^{\text{raw}}$ .

$M^{\text{raw}}$ , however, still requires additional modification. Let  $\mathcal{N}(B, A)$  represent the event that  $B$  is the nearest object to  $A$  in the shelf, and let  $S_A$  denote the event that object  $A$  is in the shelf. The affinity matrix should provide the probability that  $B$  is the nearest object to  $A$  given that both are present (but not necessarily visible) in the scene:

$$P(\mathcal{N}(B, A) | S_A, S_B) = \frac{P(\mathcal{N}(B, A), S_B | S_A)}{P(S_B | S_A)} \quad (1)$$

The affinity matrix, however, gives  $P(\mathcal{N}(B, A), S_B | S_A)$ , which differs from the desired quantity by a normalizing constant. This causes the objects corresponding to words that are used less frequently in the LLM training data to be incorrectly penalized. Because we assume  $S_i \perp S_j \forall i, j$ , we remedy this by using the sum of the probabilities across each column (object  $B$ ) as a proxy for the denominator to perform per-column normalization. We follow this with a per-row normalization to obtain a probability vector for each row (object  $A$ ). We also set the main diagonal of the matrix to zero probability as these elements reflect the affinity of objects with themselves, which is not required for mechanical search. This leads to matrix  $M^{\text{norm}}$ .

We only need to control the hyperparameter temperature  $\gamma$ , meant to control the “confidence” by regulating the uniformity of the language model’s predictions. For each row  $i$ ,

$$M_i \propto \exp(\gamma^{-1} \log M_i^{\text{norm}}).$$

This procedure leads to our ready-to-use affinity matrix  $M$ .

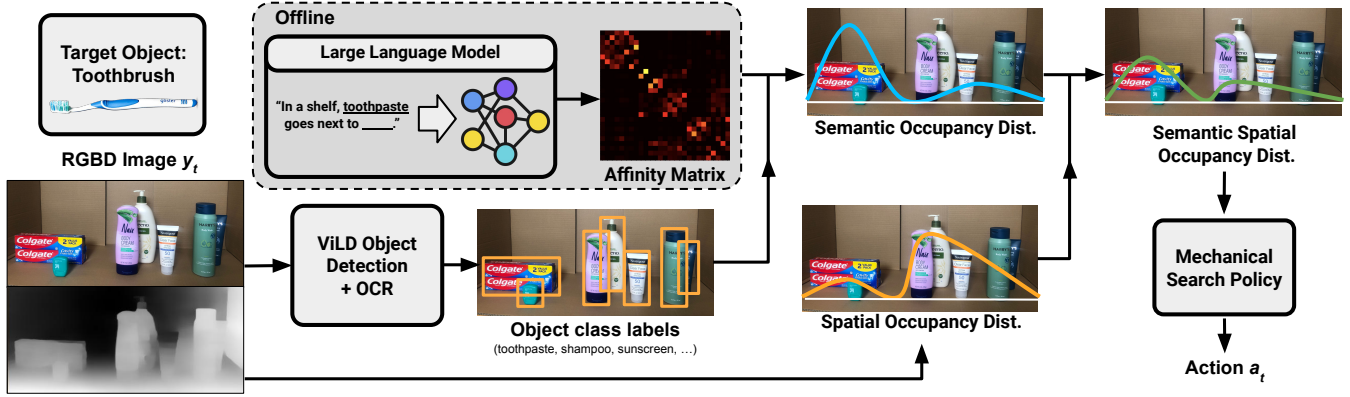


Fig. 2: System overview of Semantic Spatial Search on Shelves ( $S^4$ ). The affinity matrix is computed offline. Given an RGBD image, we use object detection combined with refinement to query the affinity matrix and construct a semantic occupancy distribution. We multiply this by a spatial occupancy distribution to use in a mechanical search policy.

## B. Object Detection Refinement

1) *OCR*: We use an object detection and segmentation model that returns object segmentation masks from an RGB input. We filter out all objects less than size  $S_{\min}$  and greater than size  $S_{\max}$ , as well as objects contained fully within other objects, in order to avoid false positives. We use the general-purpose object detector ViLD [19] to detect, segment, and classify objects in our shelf.

Because ViLD is a general-purpose detector, it cannot easily distinguish between objects belonging to the same domain (e.g., Advil versus Ibuprofen). Because of this, we use OCR with Keras OCR (<https://pypi.org/project/keras-ocr/>) to improve the quality of the object detections. For each object, we concatenate the text observed on it and compute the text embedding using OpenAI Embeddings. Then, we compute the dot product between the embeddings of the concatenated text and every class label. We then normalize this probability vector by subtracting the minimum value and then adjusting the vector with some temperature. Then, we finally multiply this by the object detection probability vector.

Let  $C_i$  denote the class label of object  $\mathcal{O}_i$  (e.g., “Tylenol”) as opposed to the broader category “medication”);  $I_i$  represent the general shape, size, and color-related features of  $\mathcal{O}_i$ ; and  $T_i$  be the detected text on  $\mathcal{O}_i$ . Recall that all objects belong to some class  $C_i$ . We calculate

$$\begin{aligned}
 & P(C_i | I_i, T_i) \\
 &= \frac{P(I_i, T_i | C_i) \cdot P(C_i)}{P(I_i, T_i)} \\
 &= \frac{P(T_i | I_i, C_i) \cdot P(I_i | C_i) \cdot P(C_i)}{P(I_i, T_i)} \\
 &= \frac{P(T_i | C_i) \cdot P(I_i | C_i) \cdot P(C_i)}{P(I_i, T_i)} \\
 &= \frac{P(C_i | T_i) P(T_i)}{P(C_i)} \cdot \frac{P(C_i | I_i) P(I_i)}{P(C_i)} \cdot \frac{P(C_i)}{P(I_i, T_i)} \\
 &\propto P(C_i | T_i) P(C_i | I_i)
 \end{aligned}$$

as  $T_i$  is independent of  $I_i$  when conditioned on  $C_i$ , and  $P(C_i)$

is uniform. This illustrates that the multiplication of the OCR probabilities and the object detection probabilities can give us a refined estimate of the category probabilities.

2) *Semantics*: We further refine the object detection probabilities by using other objects in the scene which we are more confident about. We sort the object bounding boxes from most to least confident using the Shannon entropy of each distribution over object labels after OCR refinement. We then threshold the entropy values on a confidence threshold  $c$  to determine which object bounding boxes to refine. We iterate over these high-entropy bounding boxes in increasing order of entropy and refine the distribution for the  $i$ -th bounding box using the following equation:

$$P(i)' = P(i) \cdot \frac{\sum_{j=0}^{i-1} d(i, j) \cdot M_j}{\sum_{j=0}^{i-1} d(i, j)}$$

Here,  $P(i)$  is the existing class distribution for the  $i$ -th bounding box,  $d(\cdot)$  is an exponentially decaying kernel function based on distance between any two objects in the scene, and  $M_j$  is the row of the affinity matrix corresponding to the label of the  $j$ -th object. Thus, we update probabilities to be a weighted average of the affinities of known objects, weighted by the distance to the uncertain object. The kernel function we use is of the form  $d(x) = e^{-ax}$ , where  $x$  is the pixel distance between the centers of the objects and  $a$  is a hyperparameter that depends on the dimensions of the image to normalize the distance metric across different resolutions.

## C. Semantic Occupancy Distribution

Here we describe the process of converting affinities and object detections into a semantic probability distribution over possible locations of the target object.

1) *Tracking the Original Scene*: To build the semantic distribution, the system requires knowledge of object locations in the original scene  $s_0$ . Once mechanical search begins, the shelf may become semantically disorganized. One technique to avoid this issue is to freeze the semantic distribution at  $t = 0$ , but this prevents adding information about initially occluded

objects. To remedy this, we keep track of the location of every object the first time it is seen and add new objects that are later unveiled. At every step  $t$  in a rollout, we compute our semantic distribution on our most up-to-date understanding of the object classes and their locations in the original scene.

2) *Calculating the Distribution*: The semantic occupancy distribution models the probability that the target object occupies a given location, given the classes of observed objects in the scene. The semantic distribution takes the form

$$P(L_T = l \mid L_{1\dots n} = l_{1\dots n}, C_{1\dots n} = c_{1\dots n}),$$

where  $L_T$  is the location of the target object,  $L_{1\dots n}$  are the inferred positions of the *visible* objects ( $n \leq N$ , the total number of objects in the shelf), and  $C_{1\dots n}$  are the inferred classes of the visible objects (i.e., the class labels with the highest probabilities) from Section IV-B. We abbreviate this quantity as  $P(L_T = l \mid L, C)$ .

We interpret affinity values  $M_{ij}$  to be the probability of object  $j$  being the closest to object  $i$  in expectation across scenes. However, given the current scene, there may be more or less space that is nearest to a particular object, so we interpret these affinity values as being normalized per unit area. This means that the height of the semantic distribution is directly proportional to the affinity value of the nearest object. Formally, given that  $N(l)$  is a function returning the index of the object closest to location  $l = (x_l, y_l)$ ,

$$P(L_T = l \mid L, C) \propto M_{l, N(l)}.$$

In simulation experiments,  $N(\cdot)$  is computed using the 3D coordinates of the visible objects obtained from depth image. We compute the 2D semantic occupancy distribution (in the  $xy$  plane of the shelf) and reduce it to 1D by summing along camera rays. In physical experiments, to avoid errors due to noisy depth readings we compute the distribution directly in 2D, using pixel distance for  $N(\cdot)$  instead of world coordinates. As a final post-processing step to account for noise when objects are moved or bumped around slightly, we apply smoothing using a Gaussian kernel with standard deviation  $\sigma$ . The process of calculating the semantic distribution is illustrated in Figure 3.

#### D. Semantic Spatial Search on Shelves ( $S^4$ ) Algorithm

$S^4$  combine the semantic occupancy distribution with a spatial distribution and provide it as input to a mechanical search policy. We use the method from Huang et al. [21] to learn a spatial occupancy distribution from a depth image of the scene. This distribution estimates where the target object can be based on possible occlusions of the known dimensions of the target object. We multiply this spatial occupancy distribution element-wise with the semantic occupancy distribution from Section IV-C. This weights the spatial distribution with where the object is semantically likely to be. We then use the Distribution Area Reduction (DAR) policy from Huang et al. [21] with the synthesized distribution to perform mechanical search. A full overview of  $S^4$  is shown in Figure 2.

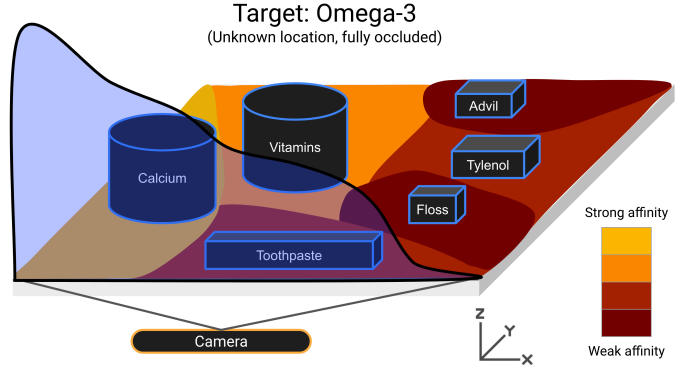


Fig. 3: Here we have an example scene where the target is Omega-3 and the visible objects are labeled. We illustrate the process of calculating the 2D semantic distribution ( $xy$ -plane of the shelf) and then projecting to a 1D semantic distribution (shaded blue in the  $xz$ -plane), as described in Section IV-C.

## V. EXPERIMENTS

In this section, we evaluate (1) the quality of affinity matrices generated by different LLMs via comparison to the Google Product Taxonomy (Section V-A), (2) ablations of key components of the object detection system such as OCR (Section V-C), and (3) the effect of LLM-based semantics on the speed of mechanical search in simulation and physical environments (Sections V-D and V-E).

### A. Affinity Matrix

The choice of LLM affects the values in the affinity matrix. In order to compare different LLMs and quantitatively evaluate the quality of affinity matrices, we use the open-source Google Product Taxonomy [5] as the “ground truth” matrix. In the pharmacy domain, we use the following 6 categories and items from the taxonomy:

- 1) Supplements: vitamins, fish oil, omega-3, calcium, probiotics, protein powder, COQ10, anthocyanin
- 2) Hair Care: shampoo, conditioner
- 3) Oral Care: toothpaste, toothbrush, dental floss
- 4) Cosmetics: face wash, sunscreen, lotion, hand cream, body wash
- 5) Medication: aspirin, tylenol, ibuprofen, advil, pain relief
- 6) Outliers: shaving cream, eye drops, deodorant, band-aid

For the ground-truth matrix, all elements in a category are given uniform affinities to each other, and each row is normalized to sum to 1.0 probability. Note that each item in the “outliers” category (e.g., eye drops) does not belong to any of the other 5 categories and is treated as its own category. With the categories listed in order along both axes of the matrix, the ground truth affinity matrix has a block-diagonal structure with a uniform block for each category (Figure 4A). We evaluate the following LLMs and embedding models off-the-shelf, without finetuning: BERT [10], CLIP [32], embeddings from the OpenAI API [13], OPT-13B [16], and PaLM. For LLMs, we generate affinity matrices as described in IV-A with  $\gamma = 1$ , and for embedding models we take the dot product of the embeddings of the object names and optimize

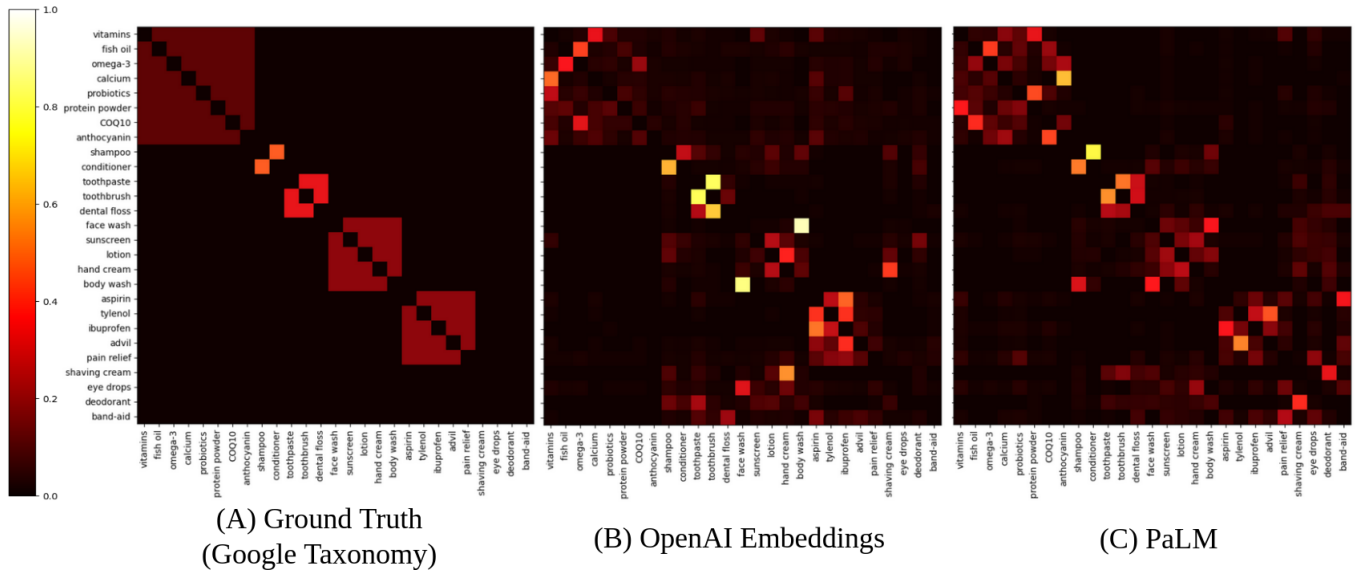


Fig. 4: Ground truth affinity matrix and affinity matrices generated by OpenAI Embeddings and PaLM. The matrices are able to roughly capture the block diagonal structure of the ground truth matrix.

the  $\gamma$  to minimize the Jensen-Shannon Distance (JSD) [27] to the ground truth. JSD measures the similarity between two probability distributions, so we measure the similarity between each row of the affinity matrix and the corresponding row of the ground truth. Then, we average across the rows to get the average distance from each object’s probability distribution to that object’s ground truth. We observe that the choice of LLM has a significant impact on the affinity matrix (Table I), and that the LLMs can approximately recover the block diagonal structure of the ground truth matrix (Figure 4). PaLM attains the highest accuracy, with a 44.6% improvement over a uniform affinity matrix.

TABLE I: Affinity matrix results. We report the average Jensen-Shannon Distance (JSD) between each row of the affinity matrix and the ground truth matrix, as well as the percentage improvement over the uniform JSD (i.e., (uniform JSD - method JSD) / uniform JSD).

Method	JSD ( $\downarrow$ )	% Improvement ( $\uparrow$ )
Uniform	0.65	N/A
BERT Embedding	0.64	1.5
CLIP Embedding	0.52	20.0
OpenAI Embedding	0.43	33.8
OPT-13B	0.38	41.5
PaLM	<b>0.36</b>	<b>44.6</b>

### B. Semantic Scene Generation

We consider three shelf domains to apply our method: a pharmacy, an industrial kitchen, and an office. We select 27, 24, and 40 representative objects respectively in these domains from the Google Product Taxonomy [5]. We provide the full lists of objects in the appendix. We use the taxonomy as a ground truth reference for producing realistic semantically arranged scenes in simulation and physical experiments. Both simulation and real experiments take place in a  $0.8\text{ m} \times 0.35\text{ m} \times 0.57\text{ m}$  shelf.

The taxonomy defines a tree where each category is a node and each object name is a leaf node. To create a scene with  $N$

objects in a given domain, we begin by uniformly sampling  $N$  objects without replacement from the total objects available in that domain. We then generate scenes in a top-down recursive manner using the taxonomy tree. At the root, we start with the whole shelf available to us. At each node, we split the shelf in half either horizontally or vertically with 50% probability each and recursively continue scene generation in these sub-shelves. If a node has more than 8 descendants, however, we always split the scene horizontally to avoid overcrowding resulting from the aspect ratio of the shelf. At each level of recursion, we accumulate random noise to the eventual placement of each object in the current branch, uniformly sampled from  $-2\text{ cm}$  to  $2\text{ cm}$ . At the last non-leaf node, we place all leaves in random positions within the current level’s sub-shelf. We resolve collisions by iteratively moving objects along the displacement vector between colliding objects and discard scenes where such a procedure takes longer than 1 second to run. We also discard scenes where there is no potential target object that is invisible from the camera’s perspective at the start of the rollout. We reiterate that the taxonomy is *independent* of the language models used to generate affinities. The LLMs are applicable beyond manual semantic categorizations like the Google Taxonomy, but we use this resource for evaluation purposes. The scenes for all simulation, physical, and object detection experiments are generated by this procedure.

We use approximate sizes of these items to generate collision-free scenes. In simulation, we also scale these objects down in order to be able to run experiments on the same-sized shelf, which has an effect similar to running experiments in a larger shelf where more items could originally fit. The scaling factors for the pharmacy and kitchen domains are 0.7, but 0.4 in the office domain due to overall larger objects unable to easily fit and move within a small shelf.

TABLE II: Object Detection Refinement Results. We ablate the components of our object detection system (Section IV-B) and report the mean average precision (mAP) of the predicted bounding boxes and top-K accuracy of the predicted labels.

Method	mAP ( $\uparrow$ )	Top-K Accuracy % ( $\uparrow$ )		
		k=1	k=3	k=5
<b>ViLD</b>	2.4	14.7	32.3	41.6
<b>ViLD + OCR</b>	28.9	45.0	62.0	69.5
<b>ViLD + OCR +Semantic Refinement</b>	<b>30.6</b>	<b>49.9</b>	<b>67.4</b>	<b>74.6</b>

### C. Object Detection

We test object detection performance on scenes generated through isolated perception experiments. We take RGB images of 100 scenes of the Pharmacy domain using a high-resolution camera and run three object detection methods:

- 1) **ViLD**: Off-the-shelf ViLD [19].
- 2) **ViLD + OCR**: Refinement of ViLD with OCR as described in Section IV-B.
- 3) **ViLD + OCR + Semantic Refinement**: The full object detection method in Section IV-B.

Results for this experiment are in Table II. As is standard in the computer vision literature, we report mAP (mean Average Precision) averaged over intersection-over-union (IOU) thresholds from 0.50 to 0.95 with a step size of 0.05, as well as top- $k$  classification accuracy (i.e., if the ground truth label appears in the  $k$  labels with the highest probabilities). The results show that OCR leads to a significant improvement across all metrics, with mAP improving by a factor of 12 and top-1 accuracy improving by a factor of 3. Adding semantic refinement further improves mAP by 1.7% and all of the top- $k$  accuracy metrics by approximately 5%, suggesting that LLMs can provide zero-shot improvement to object detection. Such a technique is especially useful when the data and model capacity required to learn such semantic relationships is limited.

### D. Simulation Object Retrieval Experiments

We run an extensive suite of experiments using the same simulator as prior work in mechanical search [21]. In simulation experiments, we consider three domains: a pharmacy, an industrial kitchen, and an office. We assume perfect object detection and thus do not render the physical appearance of the objects. We use a grid search on the average number of actions required in the pharmacy domain with 15 objects to tune the Gaussian smoothing  $\sigma$  to be 50 pixels and  $\gamma$  for PaLM to be 1 and for OpenAI Embeddings to be 0.004. We use the same parameters for the other two domains.

For each domain, we generate scenes with the procedure from Section V-B with various numbers of objects:  $N = 12, 15, 18,$  and  $21$ . We generate 200 scenes for each value of  $N$ . We also test shelves that are *not* semantically organized, with all objects placed randomly (denoted as RAND). We discard scenes where the target object starts out visible, resulting in just under 200 scenes for each value of  $N$ . Termination occurs when at least  $X = 1\%$  of the target object becomes visible. The reason for the low threshold is that the DAR policy has trouble making progress on a partially revealed

target object [20], which may dilute the comparison between different methods for generating semantic distributions.

We test the following algorithms on each type of scene:

- 1) **Spatial NN**: Mechanical search with the learned spatial occupancy distribution from [20]. No semantic information is used.
- 2) **S<sup>4</sup> (Embeddings)**: S<sup>4</sup> using the affinity matrix built with OpenAI Embeddings [13] and the same spatial distribution model as 1).
- 3) **S<sup>4</sup> (PaLM)**: S<sup>4</sup> using the affinity matrix built with PaLM and the same spatial distribution model as 1).

We report the following metrics in simulation and physical experiments:

- 1) **Successes**: The ratio of trials where the target object is found (without running out of actions or hitting the maximum action limit ( $2 \cdot N$ )) to the total number of trials.
- 2) **Number of actions**: The mean and standard error of the number of actions required to reveal the target object.

We report results for all numbers of objects  $N$  in Table III, semantically arranged versus randomly arranged scenes in Table IV, and the results averaged across all values of  $N$  in Table V. In the pharmacy domain, S<sup>4</sup> (PaLM) outperforms both S<sup>4</sup> (Embeddings), while also beating Spatial NN across various values of  $N$  in terms of success rate (by an additional 30/741 scenes) and average number of actions required (by 32.4%). A point of note is that the action differential percentage grows as the number of objects increases. At 21 objects, Spatial NN requires 8.24 actions on average, whereas S<sup>4</sup> requires just 5.47. This trend agrees with intuition that it is unscalable to search large environments with no semantic intuition.

In the kitchen domain, S<sup>4</sup> (Embeddings) and S<sup>4</sup> (PaLM) perform similarly to each other but both outperform Spatial NN significantly once again, improving the success rate and improving the number of actions required by approximately 27%. We hypothesize that the embeddings here are better able to approximate physical proximity between kitchen objects as the categories are distinct enough such that nearby objects in the embedding vector space would also be found closer together in simulated shelves.

For the office experiments, we see that S<sup>4</sup> (PaLM) consistently has the highest success rate starting at  $N = 15$  and higher. Overall, it achieves a 12% reduction in the number of actions and increases the success rate by 23/753 scenes. We hypothesize that this lower improvement is due to a majority of the office environment consisting of generic office supplies which do not have a clear semantic categorization, making semantic search less effective. S<sup>4</sup> (Embeddings) is not effective in reducing the number of actions required in this setting. We believe that this is because embeddings are not able to capture subtle differences between categories as well as the LLM is.

In Table IV, we observe that when scenes are *not* semantically arranged, S<sup>4</sup> (PaLM) has comparable performance to Spatial NN in all three domains despite having a slightly lower success rate. However, the performance of S<sup>4</sup> (Embed-

TABLE III: Simulation Experiment Results.

Pharmacy Domain								
	12 objects		15 objects		18 objects		21 objects	
	Successes	# Actions	Successes	# Actions	Successes	# Actions	Successes	# Actions
Spatial NN	168/190	4.06 ± 0.23	160/186	5.17 ± 0.28	144/188	5.78 ± 0.44	104/177	8.24 ± 0.67
S <sup>4</sup> (Embed.)	<b>176/190</b>	2.90 ± 0.18	159/186	3.77 ± 0.26	146/188	5.05 ± 0.42	110/177	5.69 ± 0.54
S <sup>4</sup> (PaLM)	<b>176/190</b>	<b>2.66 ± 0.14</b>	<b>162/186</b>	<b>3.26 ± 0.19</b>	<b>150/188</b>	<b>4.25 ± 0.34</b>	<b>118/177</b>	<b>5.47 ± 0.43</b>
Kitchen Domain								
	12 objects		15 objects		18 objects		21 objects	
	Successes	# Actions	Successes	# Actions	Successes	# Actions	Successes	# Actions
Spatial NN	185/192	2.15 ± 0.14	182/194	2.97 ± 0.23	177/193	3.99 ± 0.29	159/191	4.36 ± 0.38
S <sup>4</sup> (Embed.)	<b>186/192</b>	<b>1.56 ± 0.08</b>	<b>188/194</b>	2.15 ± 0.15	<b>184/193</b>	3.00 ± 0.27	<b>167/191</b>	<b>3.07 ± 0.25</b>
S <sup>4</sup> (PaLM)	184/192	1.60 ± 0.10	184/194	<b>2.04 ± 0.13</b>	179/193	<b>2.97 ± 0.26</b>	163/191	3.17 ± 0.28
Office Domain								
	12 objects		15 objects		18 objects		21 objects	
	Successes	# Actions	Successes	# Actions	Successes	# Actions	Successes	# Actions
Spatial NN	172/194	2.60 ± 0.18	152/188	4.15 ± 0.38	136/190	4.64 ± 0.37	115/181	5.86 ± 0.56
S <sup>4</sup> (Embed.)	<b>173/194</b>	3.01 ± 0.22	152/188	3.80 ± 0.31	140/190	4.78 ± 0.44	115/181	<b>5.33 ± 0.50</b>
S <sup>4</sup> (PaLM)	172/194	<b>2.33 ± 0.13</b>	<b>161/188</b>	<b>3.50 ± 0.31</b>	<b>142/190</b>	<b>3.75 ± 0.32</b>	<b>123/181</b>	5.50 ± 0.49

TABLE IV: Simulation Experiment: Performance in Non-Semantic (RAND) Scenes with 15 objects. “RAND” refers to randomly arranging the objects in the scene as opposed to semantically arranging them with the procedure in Section V-B.

	Pharmacy		Kitchen		Office	
	Successes	# Actions	Successes	# Actions	Successes	# Actions
Spatial NN	170/190	4.65 ± 0.29	<b>164/189</b>	4.14 ± 0.30	<b>140/173</b>	4.34 ± 0.32
S <sup>4</sup> (Embed.)	<b>172/190</b>	5.35 ± 0.31	162/189	4.70 ± 0.31	135/173	4.74 ± 0.32
S <sup>4</sup> (PaLM)	169/190	<b>4.62 ± 0.25</b>	157/189	<b>3.95 ± 0.29</b>	138/173	<b>3.85 ± 0.35</b>

TABLE V: Simulation Experiment Results in Table III averaged over number of objects, also reported with % Reduc., percentage reduction in actions from Spatial NN.

	Pharmacy Domain			Kitchen Domain			Office Domain		
	Successes	# Actions	% Reduc.	Successes	# Actions	% Reduc.	Successes	# Actions	% Reduc.
Spatial NN	576/741	5.56 ± 0.20	N/A	703/770	3.32 ± 0.14	N/A	575/753	4.14 ± 0.19	N/A
S <sup>4</sup> (Embed.)	591/741	4.18 ± 0.17	24.8	<b>725/770</b>	2.43 ± 0.10	26.8	580/753	4.10 ± 0.18	0.9
S <sup>4</sup> (PaLM)	<b>606/741</b>	<b>3.76 ± 0.14</b>	<b>32.4</b>	710/770	<b>2.42 ± 0.10</b>	<b>27.1</b>	<b>598/753</b>	<b>3.63 ± 0.16</b>	<b>12.3</b>

dings) degrades more significantly. Ultimately, results with S<sup>4</sup> (PaLM) indicate that semantic spatial search can perform as well as pure spatial search as long the scene is not adversarial (e.g., the target object is located at a very unlikely location in an otherwise semantically arranged shelf).

Overall, the results suggest that S<sup>4</sup> (PaLM) can accelerate mechanical search compared to the spatial distribution in semantically arranged environments by 32.4%, 27.1%, and 12.3% in the pharmacy, kitchen, and office domains respectively, while improving success rates.

### E. Physical Object Retrieval Experiments

We use the Kinova Gen2 robot fitted with a 3D-printed “bluction” (blade and suction) tool, as in [21]. We use an Intel RealSense depth camera mounted on the tool to provide RGB and depth observations. For physical experiments, we focus on the pharmacy domain. For these experiments, we use 3 scenes each of  $N = 7, 8, 9,$  and  $10$  objects for a total of 12 scenes and a threshold visibility of  $X = 50\%$ . See Figure 5 for the physical setup.

Because the RealSense camera is not able to capture the fine details of the text on the objects when observing the entire scene at resolution  $640 \times 480$  pixels, we perform a three-stage



Fig. 5: Physical setup with a cardboard shelf, pharmacy objects, Kinova Gen2 robot, a bluction tool [21] for extracting objects in the shelf, and an Intel RealSense RGBD camera mounted on the bluction tool.

scan of the scene by moving the end-effector to 3 adjacent positions, all of which are closer to the shelf, where the text is more easily readable. At each of these poses, we take a picture of the scene, project the known world position of the objects to the new camera frame, identify text with OCR, and assign each text detection to the object it is contained in. If there are detections on the same object from multiple scan locations, we use the OCR that has the lowest entropy for its distribution, a measure of confidence. During the physical



experiments rollouts, when the action given by the policy causes unintentional toppling or a missed grasp due to depth sensor noise, we reset the object to undo the action and run the policy again.

We evaluate the following algorithms in physical experiments:

- 1) **Spatial NN**: Same as in simulation.
- 2) **S<sup>4</sup> (PaLM)-Heuristic**: Due to the cost of deploying neural networks in the real world, we test replacing the Spatial NN in S<sup>4</sup> with a simple geometric heuristic: summing the bitwise OR of all the segmentation masks in the image along the  $y$ -axis to get a 1D distribution along the  $x$ -axis.
- 3) **S<sup>4</sup> (PaLM)**: Same as in simulation.

TABLE VI: Physical Experiment Results (12 trials each). We report the average number of actions taken to reveal the target object as well as the percentage reduction in the number of actions over the spatial neural network.

Method	# Actions	% Reduc
Spatial NN	4.25 ± 0.64	N/A
S <sup>4</sup> (PaLM)-Heuristic	2.50 ± 0.53	41.2
S <sup>4</sup> (PaLM)	2.25 ± 0.46	47.1

Results are in Table VI. An identical set of 12 semantically arranged scenes (starting configurations) generated by the procedure in Section V-B is used for each method. We observe that S<sup>4</sup> significantly accelerates mechanical search, reducing the average number of actions by 47.1%. In physical experiments, the depth image has noise while in simulation we have ground truth depth information. This results in the spatial distribution in simulation being strictly better than the spatial distribution in real. This discrepancy between the quality of the spatial distribution makes the semantic distribution more critical in identifying where a target object may lie in physical experiments. Thus, S<sup>4</sup> (PaLM) outperforms the spatial distribution by a larger margin, 47.1%, in physical experiments compared to 32.5% in the simulated pharmacy domain. Moreover, although prior work has shown that the geometric heuristic does not perform as well as the Spatial NN method [20], the results suggest that it can enable comparable mechanical search times to S<sup>4</sup> (PaLM) when coupled with a semantic occupancy distribution.

## VI. LIMITATIONS AND FUTURE WORK

In this paper we present S<sup>4</sup>, a system to facilitate mechanical search in semantically arranged environments. The system has the following limitations: (1) S<sup>4</sup> cannot accelerate mechanical search in shelves that are not semantically arranged (e.g., a kitchen pantry after hosting a dinner party), (2) S<sup>4</sup> requires setting a temperature hyperparameter in the affinity matrix to mitigate the effects of unintuitive or incorrect semantic relationships, (3) semantic refinement of object detection is less effective if the object detection distribution is low-entropy but incorrect (i.e., confidently wrong).

In future work, we hope to mitigate these limitations: for instance, adding a perception module that estimates the degree of semantic arrangement in a shelf in order to autonomously

determine a temperature for spatial semantic search. We are also interested in exploring the potential applications of interactive perception [2] to this task by, for example, developing a policy that interacts with objects for the purpose of uncovering new information about the semantics of a scene. We also hope to extend S<sup>4</sup> to mechanical search in larger spaces such as homes or office buildings, where hierarchical occupancy distributions can model entire rooms (e.g., plates are likely to be found in the kitchen or dining area).

## REFERENCES

- [1] Ehud Barnea and Ohad Ben-Shahar. Contextual object detection with a few relevant neighbors. *ArXiv preprint arXiv:1711.05705*, 2017.
- [2] Jeannette Bohg, Karol Hausman, Bharathwaj Sankaran, Oliver Brock, Danica Kragic, Stefan Schaal, and Gaurav S. Sukhatme. Interactive perception: Leveraging action in perception and perception in action. *IEEE Transactions on Robotics*, 33:1273–1291, 2016.
- [3] Nicolas Carion, Francisco Massa, Gabriel Synnaeve, Nicolas Usunier, Alexander Kirillov, and Sergey Zagoruyko. End-to-end object detection with transformers. *European Conference on Computer Vision (ECCV)*, 2020.
- [4] Nicolas Carion, Francisco Massa, Gabriel Synnaeve, Nicolas Usunier, Alexander Kirillov, and Sergey Zagoruyko. Holm: Hallucinating objects with language models for referring expression recognition in partially-observed scenes. In *Proceedings of the 60th Annual Meeting of the Association for Computational Linguistics (ACL)*, 2020.
- [5] Google Merchant Center. Google product category. <https://support.google.com/merchants/answer/6324436?hl=en>. Accessed: 2023-01-31.
- [6] Lawrence Yunliang Chen, Huang Huang, Michael Danielczuk, Jeffrey Ichnowski, and Ken Goldberg. Optimal shelf arrangement to minimize robot retrieval time. *IEEE International Conference on Automation Science and Engineering (CASE)*, 2022.
- [7] Zhe Chen, Shaoli Huang, and Dacheng Tao. Context refinement for object detection. In *European Conference on Computer Vision*, 2018.
- [8] Yuchen Cui, Siddharth Karamcheti, Raj Palleti, Nidhya Shivakumar, Percy Liang, and Dorsa Sadigh. No, to the right: Online language corrections for robotic manipulation via shared autonomy. *ACM/IEEE International Conference on Human-Robot Interaction (HRI)*, 2023.
- [9] Michael Danielczuk, Andrey Kurenkov, Ashwin Balakrishna, Matthew Matl, David Wang, Roberto Martin-Martin, Animesh Garg, Silvio Savarese, and Ken Goldberg. Mechanical search: Multi-step retrieval of a target object occluded by clutter. In *2019 International Conference on Robotics and Automation (ICRA)*, 2019.
- [10] Jacob Devlin, Ming-Wei Chang, Kenton Lee, and Kristina Toutanova. Bert: Pre-training of deep bidirec-

- tional transformers for language understanding. *ArXiv preprint arXiv:1810.04805*, 2019.
- [11] Santosh K. Divvala, Derek Hoiem, James H. Hays, Alexei A. Efros, and Martial Hebert. An empirical study of context in object detection. In *2009 IEEE Conference on Computer Vision and Pattern Recognition*, pages 1271–1278, 2009.
- [12] Aakanksha Chowdhery et al. Palm: Scaling language modeling with pathways. *arXiv preprint arXiv:2204.02311*, 2022.
- [13] Arvind Neelakantan et al. Text and code embeddings by contrastive pre-training. *arXiv preprint arXiv:2201.10005*, 2022.
- [14] Brian Ichter et al. Do as i can, not as i say: Grounding language in robotic affordances. In *6th Annual Conference on Robot Learning*, 2022.
- [15] Rishi Bommasani et al. On the opportunities and risks of foundation models. *ArXiv preprint arXiv:2108.07258*, 2021.
- [16] Susan Zhang et al. Opt: Open pre-trained transformer language models. *ArXiv preprint 2205.01068*, 2022.
- [17] Tom B. Brown et al. Language models are few-shot learners. *ArXiv preprint arXiv:2005.14165*, 2020.
- [18] Wenlong Huang et al. Inner monologue: Embodied reasoning through planning with language models. *arXiv preprint arXiv:2207.05608*, 2022.
- [19] Xiuye Gu, Tsung-Yi Lin, Weicheng Kuo, and Yin Cui. Open-vocabulary object detection via vision and language knowledge distillation. *International Conference on Learning Representations (ICLR)*, 2021.
- [20] Huang Huang, Marcus Dominguez-Kuhne, Vishal Satish, Michael Danielczuk, Kate Sanders, Jeffrey Ichnowski, Andrew Lee, Anelia Angelova, Vincent Vanhoucke, and Ken Goldberg. Mechanical search on shelves using lateral access x-ray. In *2021 IEEE/RSJ International Conference on Intelligent Robots and Systems (IROS)*, pages 2045–2052, 2021.
- [21] Huang Huang, Michael Danielczuk, Chung Min Kim, Letian Fu, Zachary Tam, Jeffrey Ichnowski, Anelia Angelova, Brian Ichter, and Ken Goldberg. Mechanical search on shelves using a novel “bluction” tool. *IEEE International Conference on Robotics and Automation (ICRA)*, 2022.
- [22] Huang Huang, Letian Fu, Michael Danielczuk, Chung Min Kim, Zachary Tam, Jeffrey Ichnowski, Anelia Angelova, Brian Ichter, and Ken Goldberg. Mechanical search on shelves with efficient stacking and destacking of objects. *International Symposium on Robotics Research (ISRR)*, 2022.
- [23] Yiding Jiang, Shixiang Shane Gu, Kevin P. Murphy, and Chelsea Finn. Language as an abstraction for hierarchical deep reinforcement learning. *Conference on Neural Information Processing Systems (NeurIPS)*, 2019.
- [24] Sezer Karaoglu, Jan Gemert, and T. Gevers. Object reading: Text recognition for object recognition. volume 7585, 10 2012. ISBN 978-3-642-33884-7. doi: 10.1007/978-3-642-33885-4\_46.
- [25] Andrey Kurenkov, Roberto Martín-Martín, Jeff Ichnowski, Ken Goldberg, and Silvio Savarese. Semantic and geometric modeling with neural message passing in 3d scene graphs for hierarchical mechanical search. *International Conference on Robotics and Automation (ICRA)*, 2021.
- [26] Jacky Liang, Wenlong Huang, Fei Xia, Peng Xu, Karol Hausman, Brian Ichter, Peter R. Florence, and Andy Zeng. Code as policies: Language model programs for embodied control. *ArXiv preprint arXiv:2209.07753*, 2022.
- [27] J. Lin. Divergence measures based on the shannon entropy. *IEEE Transactions on Information Theory*, 37 (1):145–151, 1991. doi: 10.1109/18.61115.
- [28] Corey Lynch and Pierre Sermanet. Language conditioned imitation learning over unstructured data. *Robotics: Science and Systems (RSS)*, 2021.
- [29] Corey Lynch, Ayzaan Wahid, Jonathan Tompson, Tianli Ding, James Betker, Robert K. Baruch, Travis Armstrong, and Peter R. Florence. Interactive language: Talking to robots in real time. *ArXiv preprint arXiv:2210.06407*, 2022.
- [30] Dipendra Kumar Misra, John Langford, and Yoav Artzi. Mapping instructions and visual observations to actions with reinforcement learning. In *Conference on Empirical Methods in Natural Language Processing (EMNLP)*, 2017.
- [31] Suraj Nair, Eric Mitchell, Kevin Chen, Brian Ichter, Silvio Savarese, and Chelsea Finn. Learning language-conditioned robot behavior from offline data and crowd-sourced annotation. In *Conference on Robot Learning (CoRL)*, 2021.
- [32] Alec Radford, Jong Wook Kim, Chris Hallacy, Aditya Ramesh, Gabriel Goh, Sandhini Agarwal, Girish Sastry, Amanda Askell, Pamela Mishkin, Jack Clark, Gretchen Krueger, and Ilya Sutskever. Learning transferable visual models from natural language supervision. In *International Conference on Machine Learning (ICML)*, 2021.
- [33] Pratyusha Sharma, Balakumar Sundaralingam, Valts Blukis, Chris Paxton, Tucker Hermans, Antonio Torralba, Jacob Andreas, and Dieter Fox. Correcting robot plans with natural language feedback. *Robotics: Science and Systems (RSS)*, 2022.
- [34] Mohit Shridhar, Lucas Manuelli, and Dieter Fox. Cliport: What and where pathways for robotic manipulation. *Conference on Robot Learning (CoRL)*, 2021.
- [35] Mohit Shridhar, Lucas Manuelli, and Dieter Fox. Perceiver-actor: A multi-task transformer for robotic manipulation. *Conference on Robot Learning (CoRL)*, 2022.
- [36] Hwanjun Song, Deqing Sun, Sanghyuk Chun, Varun Jampani, Dongyoon Han, Byeongho Heo, Wonjae Kim, and Ming-Hsuan Yang. ViDT: An efficient and effective fully transformer-based object detector. In *International Conference on Learning Representations*, 2022.
- [37] Ashish Vaswani, Noam Shazeer, Niki Parmar, Jakob

Uszkoreit, Llion Jones, Aidan N. Gomez, Lukasz Kaiser, and Illia Polosukhin. Attention is all you need. In *Neural Information Processing Systems (NeurIPS)*, 2017.

## VII. APPENDIX

### A. Object Lists

#### Pharmacy Domain

- vitamins
- fish oil
- omega-3
- calcium
- probiotics
- protein powder
- COQ10
- anthocyanin
- shampoo
- conditioner
- toothpaste
- toothbrush
- dental floss
- face wash
- sunscreen
- lotion
- hand cream
- body wash
- aspirin
- tylenol
- ibuprofen
- advil
- pain relief
- shaving cream
- eye drops
- deodorant
- band-aid

#### Kitchen Domain

- spoon
- ladle
- spatula
- tongs
- whisk
- fork
- peeler
- grater
- saucepan
- frying pan
- salt
- pepper
- cumin
- coriander
- basil
- turmeric
- parsley
- oregano
- sugar
- flour
- cornstarch
- oats
- quinoa
- rice

#### Office Domain

- pen
- pencil
- highlighter
- sticky note
- binder paper
- printer paper
- index card
- paper clip
- rubber band
- stapler
- staples
- tape dispenser
- 3-hole punch
- dry erase marker
- sharpie
- label maker
- notebook
- eraser
- white-out
- calculator
- thumbtack
- pencil sharpener
- bubble wrap
- styrofoam
- packing tape
- shipping boxes
- ethernet cable
- modem
- router
- network card
- network bridge
- headphones
- speakers
- aux cable
- microphone
- keyboard
- mouse
- USB adapter
- hard drive
- flash drive